Chapter 5: Evidence for the Involvement of CD44 in the Induction of Vascular Leak Syndrome (VLS)

Abstract

In a recent study we noted that cytotoxic lymphocytes were involved in endothelial cell injury following IL-2 therapy, leading to the induction of vascular leak syndrome (VLS). At sites of chronic inflammation seen during infections, autoimmunity, graft-versus-host response and cytokine therapy, endothelial cell injury is known to occur, the exact mechanism of which is unknown. In the current study we used IL-2 induced VLS as a model to investigate the role of CD44 in endothelial cell injury. Administration of IL-2 into wild-type mice triggered significant VLS in the lungs and liver. In contrast, in CD44-KO mice, IL-2-induced VLS was markedly reduced in the lungs and liver. IL-2 treated wild-type and CD44-KO mice had similar levels of perivascular infiltration with lymphocytes. This suggested that the decrease in VLS was not due to the inability of lymphocytes to migrate to the lung and liver. Ultrastructural studies demonstrated extensive endothelial cell damage in the lungs and liver of IL-2-treated wild-type mice. Interestingly, IL-2 treated CD44-KO mice showed very little damage. The VLS seen in wild-type mice treated with IL-2 was blocked by administration of $F(ab\grave{})_2$ fragments of antibodies against CD44. The current study demonstrates that CD44 plays a key role in the induction of VLS by IL-2. Blocking CD44 in vivo may offer a novel therapeutic approach to prevent endothelial cell injury by cytotoxic lymphocytes in a variety of clinical disease models.

Introduction

In a number of disease models including infections, autoimmunity, transplantation, graft-versus-host disease, severe damage to the endothelial cells leading to toxicity has been known to occur (Doherty et al.,1990; Tsukada

et al., 1993; Moyer et al., 1983; McCluskey et al.,1983; Hewicker et al., 1987). However, the exact mechanism of such endothelial cell damage is not clear. Furthermore, IL-2 therapy has been shown to be effective in the treatment of certain types of cancer, although its use is limited by toxicity resulting from endothelial cell damage and capillary leak (Bechard et al., 1989; Vial et al., 1995). Several cytokines including those used as hematopoeitic growth factors, have been shown to trigger toxicity resulting in increased capillary leak, also known as vascular leak syndrome (VLS) (Vial et al., 1995). It has been widely speculated that immune cells, particularly the cytotoxic lymphocytes may play an important role in endothelial cell damage.

CD44 is a cell adhesion molecule with proposed functions in extracellular matrix (ECM) binding, cell migration, lymphopoiesis, and lymphocyte homing (Lesley et al., 1993). CD44 is a diverse family of molecules produced by alternate splicing of multiple exons of a single gene and by different posttranslational modifications in different cell types (Lesley et al., 1993). It is a widely distributed cell surface glycoprotein whose principal ligand has been identified as hyaluronic acid (HA), a major component of the extracellular matrix (ECM).

We and others have shown that activated cytotoxic T lymphocytes (CTL), natural killer (NK)/lymphokine activated killer (LAK) cells and the cytotoxic double-negative T cells, express increased levels of CD44 and mediate efficient lysis of target cells when activated through CD44 (Seth et al., 1991; Tan et al., 1993; Rosenberg et al., 1985). Inasmuch as CD44 also plays a major role in the lymphocyte adhesion to the endothelial cells, we have hypothesized that dysregulation in the interaction between cytolytic lymphocytes expressing CD44 and the endothelial cells bearing the appropriate ligand could lead to endothelial cell injury and VLS.

To this end, we have shown that IL-2 induced VLS is markedly decreased in mice deficient in perforin and Fas Ligand (Rafi et al., 1998),

thereby suggesting the involvement of cytotoxic lymphocytes in VLS. Also, treatment with IL-2 caused significant increase in the expression of CD44, migration and perivascular infiltration of lymphocytes in various organs and endothelial cell damage (Rafi et al., 1998).

In the current study, we further tested the hypothesis that CD44 is directly involved in the injury to the endothelial cells caused by CTL and LAK cells, during IL-2-induced VLS. To this effect, we used CD44 knockout (KO) mice and observed that such mice exhibit markedly diminished VLS following IL-2-treatment. Our data also suggest that blocking CD44 helps in reducing the IL-2-induced VLS and therefore such an approach may serve as a useful tool to prevent endothelial cell damage seen in a variety of clinical disorders.

Materials and Methods

Mice: Adult female retired breeder C57BL/6 mice were purchased from the National Institutes of Health (Bethesda, MD). CD44-knockout mice were obtained from AMGEN Institute (Toronto, Ontario) and bred in our animal facilities and screened for the CD44 mutation. The phenotype of these mice has been described elsewhere (Schmits et al., 1997).

Cell Lines: P815, a mastocytoma resistant to NK cells, was maintained *in vitro* by serial passages.

Antibodies: Monoclonal MEL-14 (lymphocyte homing receptor; rat IgG) and anti-LFA-1 (M17/4; rat IgG) were grown *in vitro* . The FITC-CD3, PE-CD44, PE-CD8 and FITC-CD4 mAbs were purchased from Pharmingen (San Diego, CA). FITC-conjugated $F(ab')_2$ fragment of goat anti-syrian hamster IgG was purchased from Jackson ImmunoResearch Laboratories, Inc (West Grove, PA). $F(ab')_2$ fragments of anti-CD44 mAbs were prepared by treatment with pepsin and passing the fragments over a protein A column (Pierce Chemical Co.) (Seth et al., 1991). Evan's Blue dye was obtained from Sigma Chemical Co.

Interleukins: Recombinant IL-2 (rIL-2) was kindly provided by Hoffman LaRoche (Nutley, NJ) and by Dr. C. Reynolds, NIH, Bethesda, MD.

Detection of CD44 mutation: Genomic DNA was obtained from the tail for PCR. Briefly, DNA was digested overnight in a digestion buffer consisting of Tris/HCL (1M), EDTA (0.5M), 10% SDS and Proteinase K (10mg/mL). The primers used for PCR were upstream of the targeting vector. To detect neo integration were 5'(606-19) 5Ì TTG AAT GTA ACC TGC CGC TAC GCA 3' and 3'(Neo-1400) 5'TAT CAG GAC ATA GCG TTG GCT ACC C 3'. To detect wild-type conditions

5’ (606-19) and 3’ (612-16) 5’ GGC CAA CTT CAT TTG GTC CAT GGT 3’ were used.

Detection of surface molecules using immunofluorescence analysis: Splenic T cells and LN cells were analyzed for LFA-1 and MEL-14 expression by staining the cells with unlabelled primary antibodies against these markers for 30 minutes on ice followed by washing three times. After washing, FITC-conjugated secondary antibody (Ab) was added to detect the presence of LFA-1 and Mel-14. The secondary Ab consisted of FITC-conjugated anti-rat IgG $F(abÌ)_2$ (Cappel). Negative controls consisted of fluorescence obtained by staining cells with FITC-conjugated secondary Ab. CD3, CD4, CD44 and CD8 expression was detected by staining the cells with PE or FITC-conjugated antibody against these markers 30 minutes on ice followed by washing three times. Nonspecific staining was blocked by incubation of cells with 0.5% normal mouse serum for 30 minutes prior to staining with labeled antibody. Next, 10,000 cells were analyzed by a flow cytometer (Epics V, Model 752, Miami, FL).

Quantitation of Vascular Leak Syndrome: Vascular leak was studied by measuring the extravasation of Evans blue which when given intravenously this dye binds plasma proteins, particularly to albumin and following extravasation, can be detected in various organs as described previously (Udaka et al., 1970). Groups of 5 mice were injected intraperitoneally with 65,000 rIL-2 or phosphate buffered saline (PBS) as a control, thrice a day for 3 days. On day 4, they received one injection in the morning and two hours later, were injected intravenously with 0.1 milliliters of 1% Evans blue in PBS. After two hours, the mice were bled to death under anesthesia, and the heart was perfused with heparin in PBS as described previously (Li, 1994). The lungs, liver and spleen were harvested, placed in formamide at 37°C overnight. The Evans blue in the

organs was quantitated by measuring the absorbance of the supernatant at 650 nm with a spectrophotometer. The VLS seen in IL-2 treated mice was expressed as percent increase in the extravasation when compared to the PBS-treated controls and was calculated as:

$$\frac{(\mu g \text{ in the organ of IL-2 treated mice} - \mu g \text{ in the organ of PBS treated controls})}{(\mu g \text{ in the organ of PBS treated control})} \times 100$$

Each mouse was individually analyzed for vascular leak and the data from 5 mice were expressed as mean±SEM percent increase in VLS in IL-2 treated mice when compared to the PBS treated controls.

Histology: For histopathological studies, groups of 5 separate mice were injected with IL-2 or PBS as described earlier and on day 4, lungs and liver were fixed in 10% formalin solution. The organs were embedded in paraffin, sectioned and stained with hematoxylin and eosin. Perivascular infiltration was scaled by counting the number of lymphocytes infiltrating the vessel and averaging the minimum and maximum range for each group. Three samples were used for lung and ten samples for the liver.

Electron microscopy studies: Tissue samples were fixed in 5% Glutaldehyde/ 4.4% Formaldehyde/ 2.75% Picric Acid in 0.05M Sodium Cacodylate buffer, pH 7.4. Samples were washed in a sodium cacodylate buffer. Samples were post-fixed in osmium tetroxide and embedded in Polybed 812 resin and studied with an electron microscope.

Cytotoxicity: The ability of splenic T cells to lyse various tumor targets was tested using ^{51}Cr-release assays. Briefly, $5x10^6$ target cells (P815) were labeled with $^{51}NaCrO_4$ by incubating at 37°C for 1 hour. Varying ratios of effector:target cells in triplicate were added in 96-well round-bottom plates (Falcon 3910,

Becton Dickinson, Lincoln Park, NJ) and incubated for 4 hours at 37°C. Spontaneous release was measured by incubating the ^{51}Cr-labeled targets alone, and total release was determined by incubating the labeled target cells with 0.1M SDS. The supernatants were harvested after 4 hours and radioactivity was measured with a gamma counter (TmAnalytic, Elk Grove Village, IL)

Statistical analysis: The VLS data in different strains of mice was compared using ANOVA and $p<0.05$ were considered to be statistically significant.

Results

Detection of the CD44 mutation: To identify CD44-KO mice genomic DNA was obtained from the tail, digested overnight and used for PCR. Figure 1 depicts a representative experiment in which CD44 wild-type (+/+), heterozygous (+/-) and homozygous (-/-) mice were screened using PCR. Based on the primers used, the CD44 (+/+) mice exhibited only the 135 bp band, CD44 (+/-) showed 135 bp band and 300 bp band and CD44 (-/-) displayed only 300 bp band (Figure 5.1). To further phenotypically confirm the expression of CD44, the wild-type and CD44-KO mice were screened using flow cytometry. To this end, splenic T cells from wild-type or CD44-KO mice were stained with mAbs against CD44 either immediately or following activation with ConA. The data shown in Figure 5.2 indicated that T cells from CD44-KO mice failed to express CD44 even after activation, while, similar cells from wild-type mice expressed high levels of CD44.

Decreased proliferative response of B cells to hyaluronic acid in CD44-KO mice: Previous studies from our lab demonstrated that splenic B cells exhibit a strong proliferative response to stimulation with hyaluronate (Rafi et al., 1997). We therefore tested to see if the CD44-KO mice displayed a decreased

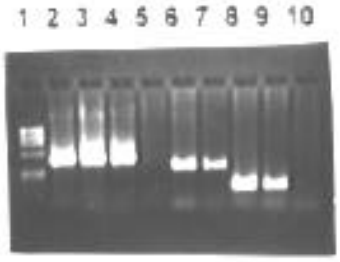

Figure 4.1: Detection of CD44-deficient mice: Genomic DNA was obtained from the tail for PCR. Briefly, DNA was digested overnight in a digestion buffer (Tris/HCL (1M), EDTA (0.5M), 10% SDS, Proteinase K (10mg/mL). Primers used for PCR were 5Ì(606-19) 5Ã TTG AAT GTA ACC TGC CGC TAC GCA 3Ì, 3Ì(Neo-1400) 5ÌTAT CAG GAC ATA GCG TTG GCT ACC C 3Ì, (WT)5Ì GGC CAA CTT CAT TTG GTC CAT GGT 3Ì. Lane 1 shows the molecular marker φX174/Hae III. Lanes 2-4 represent the β-actin control for mice 1-3 respectively. Lanes 5-7 represent the detection of CD44 mutation for mice 1-3 respectively. Lanes 8-10 represent the detection of CD44 wild-type band for mice 1-3 respectively. Homozygous CD44-knockout mice had a 300 bp band (mouse 3). Heterozygous mice had a 300 bp and 135 bp band (mouse 2). Homozygous CD44+/+ mice had only the 135 bp band (mouse 1).

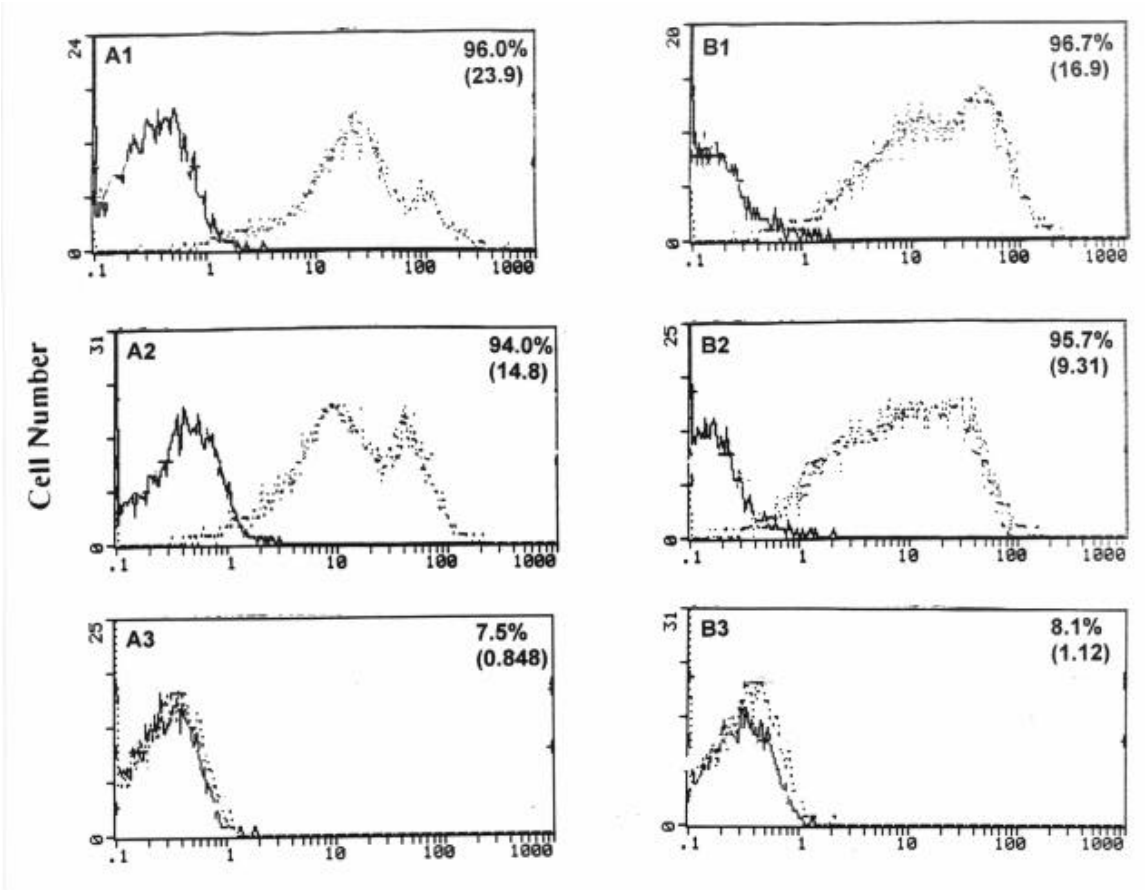

Figure 5.2: Detection of CD44 in the spleen using flow cytometry: CD44+/+ (A1, B1), CD44 +/- (A2,B2) and CD44-/- (A3, B3) mice were screened for CD44 expression before (A) and after (B) stimulation with ConA via flow cytometry. Purified splenic T cells were stained for CD44 using PE labeled CD44. The bold histogram represent autofluorescence and the broken histogram represent cells stained with PE-CD44.

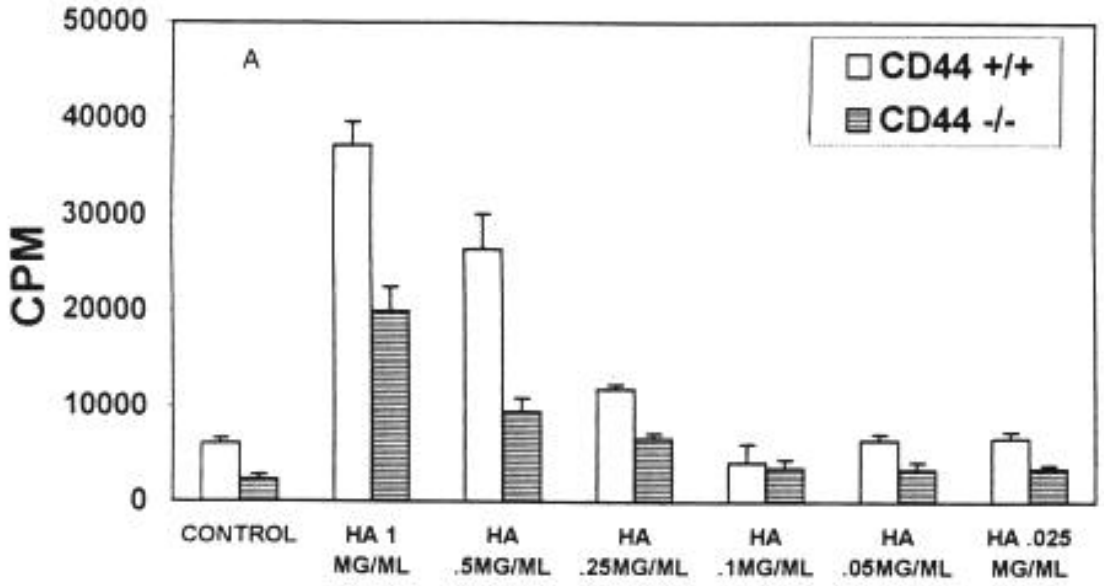

Figure 5.3: Spleen cells from CD44KO mice have a decreased response to hyaluronic acid: Spleen cells from CD44-KO mice were cultured in triplicate at a concentration of $6x10^5$ cells/well, in 96 well, flat bottom tissue culture plates in a final volume of 200 µl of complete medium per well. Medium alone (control) or hyaluronic acid was added to the wells and the cultures were incubated at 37°C for 48 hours. The cultures were pulsed with ^{3}H-thymidine (2 µCi) 6 hours before harvesting. The cells were harvested using a semiautomated cell harvester (Skatron Inc., Sterling, VA) and the labeled DNA was counted in a liquid scintillation counter.

proliferative response to HA. To this end, spleen cells were cultured in triplicate in the presence of HA for 48 hours and cell proliferation was measured. As seen in figure 5.3, CD44-ko mice displayed a dose dependent decrease in response to stimulation with HA.

Decreased VLS in CD44-KO mice: To investigate the role of CD44 in IL-2 induced VLS, groups of five wild-type or CD44-KO mice were injected with 65,000 units of IL-2 three times a day for 3 days and once on day 4. On the last day, the mice were injected with 1% Evans blue dye and VLS was studied by determining the extravasation of Evans blue in the lungs, liver and spleen.

Figure 5.4 shows a representative experiment in which the wild-type (B/6 +/+) mice displayed significant VLS following IL-2 administration in the lung and liver compared to the PBS treated group. However, in the CD44-KO mice, there was a statistically significant decrease in the lung and liver. These data suggested that CD44 may play a key role in the induction of VLS in the lung and liver.

Histopathological studies in organs exhibiting VLS: Inasmuch as CD44 is involved in lymphocyte homing to organs, histopathological studies were carried out to see if the decrease in VLS in CD44-KO mice was due to the inability of the lymphocytes to migrate to the lungs and liver. Mice were injected with PBS or IL-2 as described in Figure 5.2. On day 4, the organs were harvested and stained with hematoxylin and eosin. The PBS treated mice did not exhibit any infiltration in the lungs and liver. IL-2 treated wild-type mice had significant lymphocytic infiltration in the lungs and liver (Figure 5.5) consistent with our earlier studies (Rafi et al., 1998). The CD44-KO mice also exhibited similar levels of

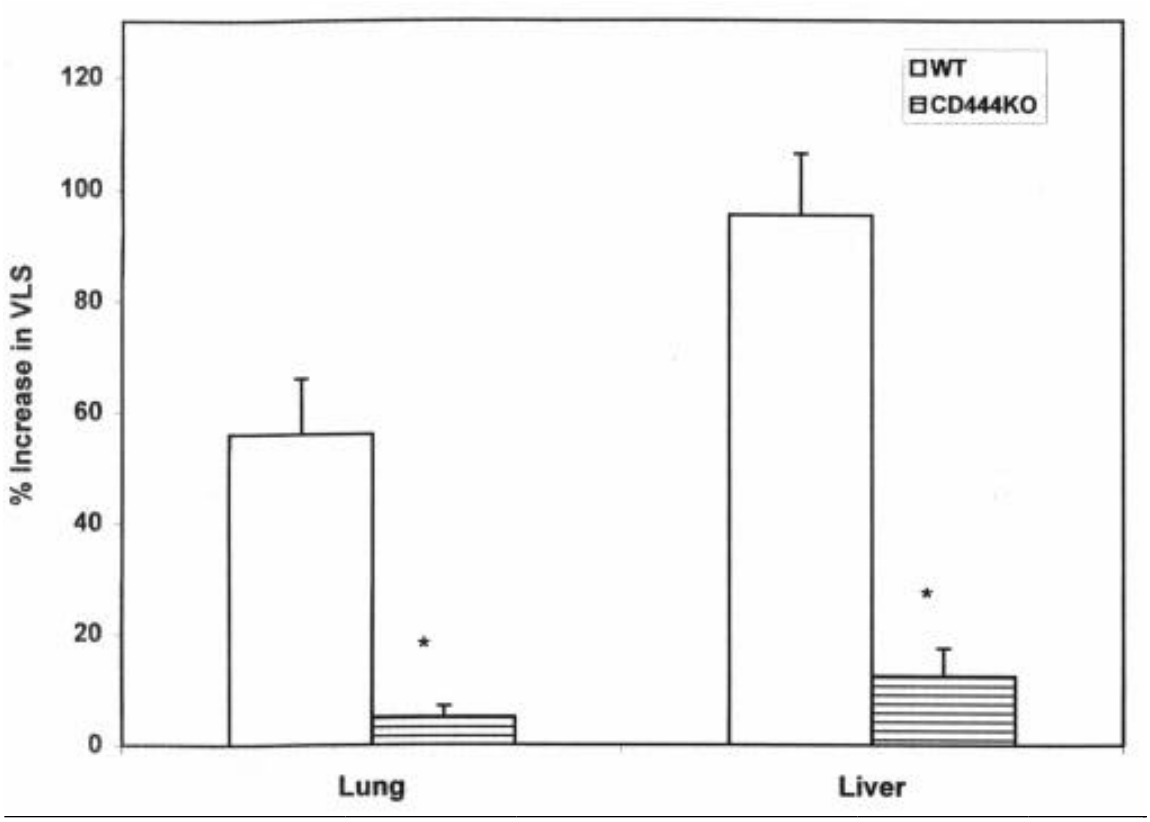

Figure 5.4: Decrease in VLS in CD44KO mice following IL-2 administration: Groups of 5 mice of C57BL/6 wild-type (+/+) and CD44KO mice were injected i.p. with 65,000 units of IL-2 three times daily for three days and once on day 4. Two hours later, the mice were injected with 1% Evans blue and VLS was studied by determining the extravasation of Evans blue dye in the lungs, liver and spleen. The vertical bars represent % increase in VLS±SEM, seen following IL-2 treatment when compared to the PBS-treated controls, as described in methods.

Figure 5.5A: Histological studies on lungs in IL-2 treated mice: Lungs from wild-type (1,2) and CD44KO (3,4) mice treated with PBS (1,3) or IL-2 (2,4) were harvested and preserved in 10% formalin solution. Sections were stained with hematoxylin and eosin. Arrows indicate perivascular infiltration consisting mostly of lymphocytes.

Figure 5.5B: Histological studies on liver in mice following IL-2 treatment: Livers from wild-type (1,2) and CD44KO (3,4) mice treated with PBS (1,3) or IL-2 (2,4) were harvested and preserved in 10% formalin solution. Sections were stained with hematoxylin and eosin. Arrows indicate perivascular infiltration consisting mostly of lymphocytes.

Table IV **Perivascular Infiltrating Lymphocytes from Wild-type and CD44KO Mice treated with IL-2**

Organ	Strain [a]	
	Wild-type	CD44KO
Lung[b]	3.85±0.75	3.0±0.34
Liver[c]	3.25±0.27	2.81±0.37

[a] Mice were injected with IL-2 to induce VLS and the organs were processed for histopathological studies as described previously. The degree of perivascular infiltration was measured by counting the number of lymphocytes infiltrating each vessel.

[b,c] The number of lymphocytes infiltrating a venule. The data represent the Mean±S.E.M. obtained from 4 samples per mouse (4 mice were analyzed for each organ).

perivascular infiltration. The degree of infiltration was also measured by counting the number of lymphocytes infiltrating each vessel and averaging the range for each group (Table IV). These results showed that IL-2 treated wild-type and CD44-KO mice had similar levels of perivascular infiltration. These data suggested that the decrease in VLS was not due to the inability of lymphocytes to migrate to the lung and liver. IL-2 treatment also caused an increase in the density expression of LFA-1 in the spleen (data not shown). The LFA-1 adhesion receptor has been shown to be involved in the cytotoxic activity in IL-2 activated NK cells (Matsumoto et al., 1998) and may be compensating for the CD44 deficiency in the CD44-KO mice.

Ultrastructural studies on of the lung and liver from mice undergoing VLS: To further corroborate that IL-2 induced VLS resulted from actual damage to the endothelial cells, ultrastructural studies of the lung (Figure 5.6) and liver (Figure 5.7) were performed. As shown in Fig 5.6 (panel 1), lungs from wild-type mice injected with PBS (control) displayed no morphological indications of damage to the endothelial cells. Similar results were seen in PBS-treated wild-type and CD44-KO groups in both the lung and liver. In contrast, following injection with IL-2, the wild-type mice demonstrated extensive damage to the basal lamina and endothelial cells. Cellular debris from former endothelial cells was found in the blood capillary lumen. Some of the endothelial cells were severely damaged with only extended cell membrane remnants remaining (Fig 5.6, panel 2). In IL-2 treated CD44-KO mice, we observed morphologically normal endothelial cells pressed against the basal lamina. The endothelial cells had intact organelles and very little morphological differences could be seen between the IL-2 treated (Figure 5.6, panel 4) and control tissues (Figure 5.6, panel 3).

There was extensive damage to the endothelial cells in the liver of wild-type mice treated with IL-2, resulting in their destruction and cellular debris in the

lumen.

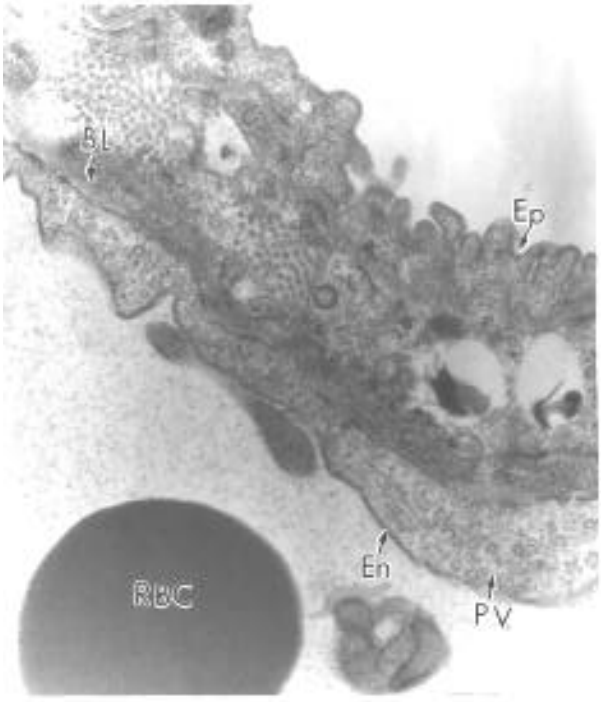

Figure 5.6 (1): Ultrastructural studies on lung in PBS treated wild-type mice: A cross section of an alveolar sac. The endothelial cells (En) lining the blood vessel are firmly anchored to the thin basal lamina (BL) and contain numerous pinocytotic vesicles (PV). A red blood cell (RBC) lies within the blood vessel lumen.

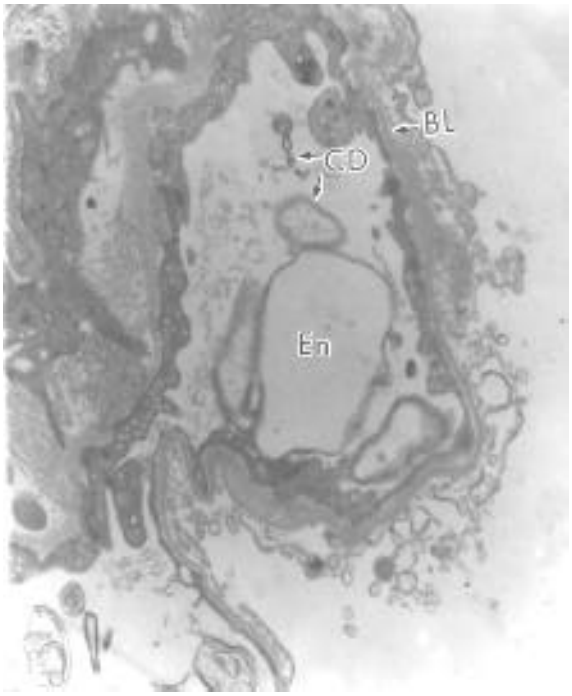

Figure 5.6 (2): Ultrastructural studies on lung in IL-2 treated wild-type mice: Cellular debris (CD) from former endothelial cells (En) is found in the blood capillary lumen. Some of the endothelial cells have been lost with only extended cell membrane remnants remaining. The basal lamina (BL) is often attenuated or absent in some areas around the capillary.

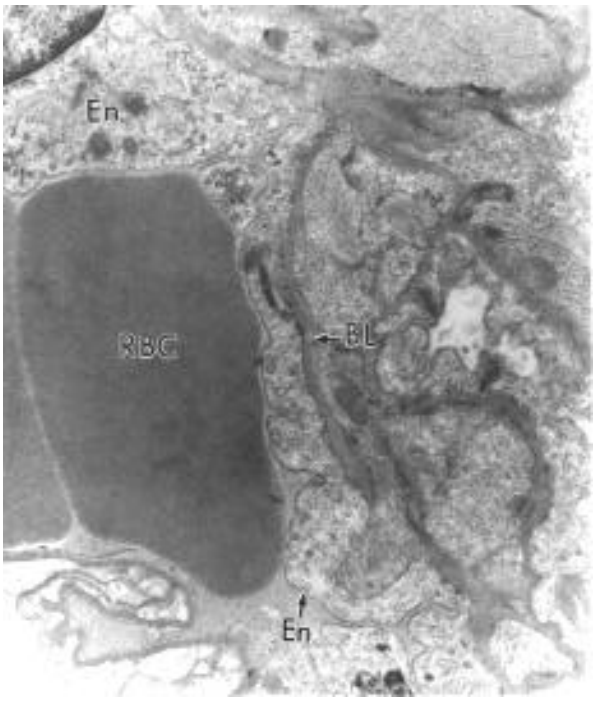

Figure 5.6 (3): Ultrastructural studies on lung in PBS treated CD44-KO mice: The endothelial cell (En) membranes and cytoplasmic contents are well defined and closely adhere to the basal lamina (BL). Two red blood cells (RBC) fill the capillary space.

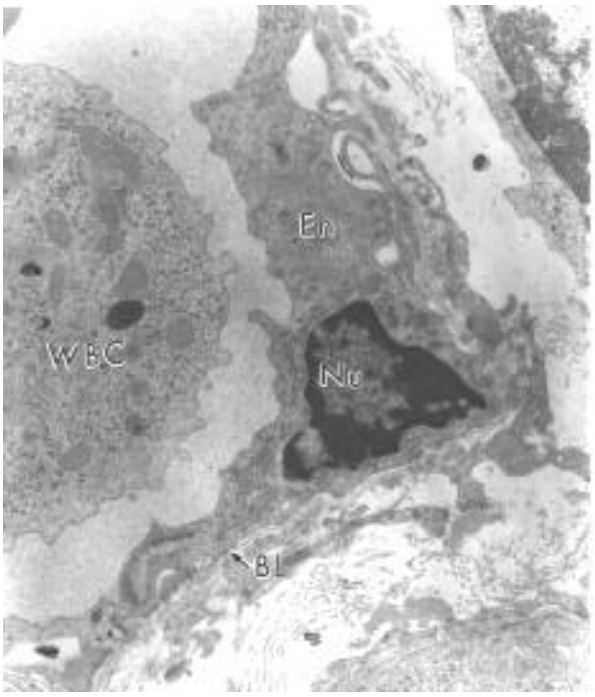

Figure 5.6 (4): Ultrastructural studies on lung in IL-2 treated CD44-KO mice: The endothelial cell (En) has an intact nucleus (Nu) and is closely apposed to an intact basal lamina (BL). A white blood cell (WBC) occupies the capillary space.

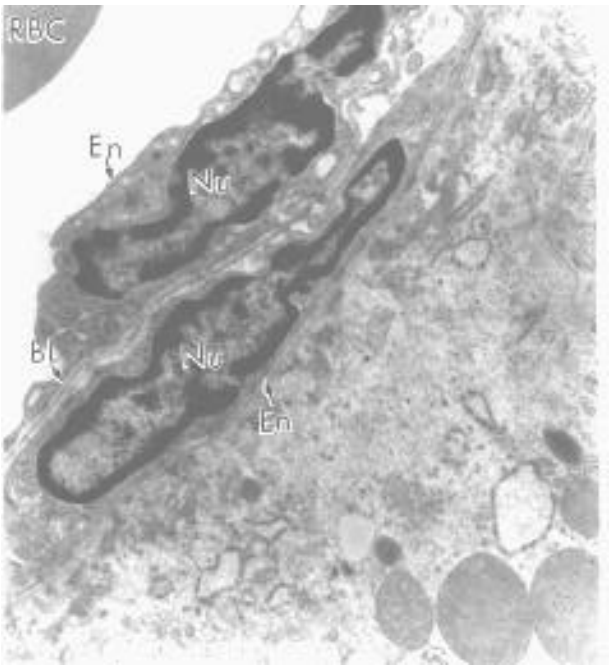

Figure 5.7 (1): Ultrastructural studies on liver in wild-type mice following PBS treatment: Endothelial cells (En) are pressed against the basal lamina (BL). The endothelial cell has a prominent nucleus (Nu) and well-defined cytoplasmic features.

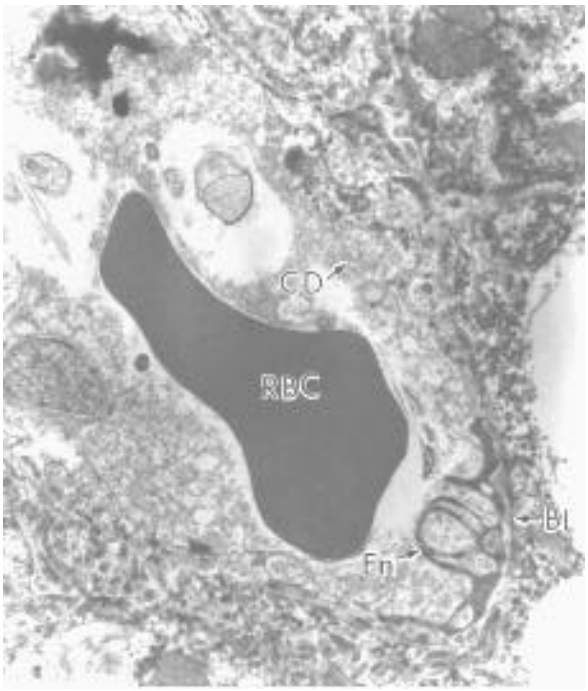

Figure 5.7 (2): Ultrastructural studies on liver in wild-type mice following IL-2 treatment: A red blood cell (RBC) lies in the capillary lumen and is surrounded by remnants of the endothelial tissue (CD). The basal lamina (BL) has also been damaged and is absent is some areas.

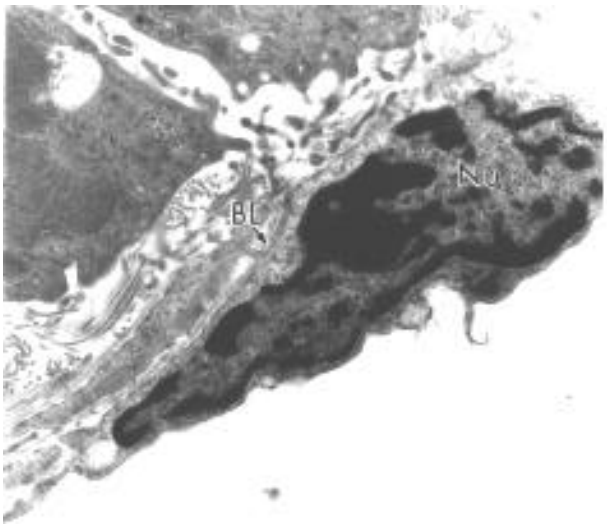

Figure 5.7 (3): Ultrastructural studies on liver in CD44-KO mice following PBS treatment: A healthy endothelial cell (En) with a well-defined nucleus (Nu) presses tightly against the basal lamina (BL).

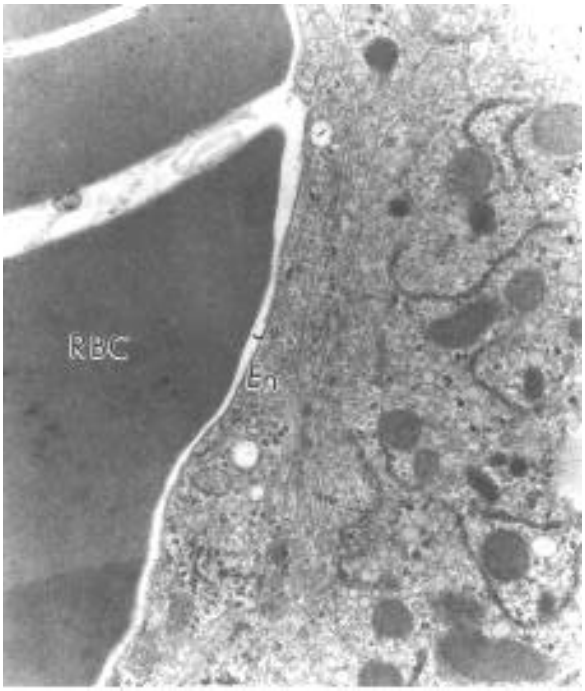

Figure 5.7 (4): Ultrastructural studies on liver in mice following IL-2 treatment: A section of liver from IL-2 treated CD44-KO mice. This section is composed of cells with normal morphology. The endothelial cells (En) and cells outside the capillary are rich in cytoplasmic organelles and normal appearing membranes.

Only remnants of the basal lamina were present (Figure 5.7, panel 2). However, in IL-2 treated CD44-Ko mice, the lungs (Figure 5.6, panel 4) and liver (Figure 5.7, panel 4) resembled the control tissues of the lung (Figure 5.6, panel 3) and liver (Figure 5.7, panel 3) and appeared morphologically normal. These results confirmed the earlier observation that IL-2 treatment induces marked VLS in wild-type but not CD44-KO mice and that the VLS resulted from actual damage to the endothelial cells as shown previously by our lab.

Use of $F(ab')_2$ Fragments of antibodies against CD44 on VLS induction in wild-type mice : To further confirm the role of CD44 in VLS, C57BL/6 wild-type mice were treated with IL-2 alone, IL-2 and 100 µg $F(ab')_2$ fragments of antibodies against CD44 (IM7) or IL-2 and rat IgG as a control. As seen in Figure 5.8a, injection of $F(ab')_2$ fragments of antibodies against CD44 (IM7) significantly inhibited VLS in the lung and liver. In contrast, injection of rat IgG as a control did not have any significant effect on VLS. The inhibition caused by anti-CD44 in VLS was dose dependent as shown in Figure 5.8. In a similar experiment using 500 µg $F(ab')_2$ fragments of antibodies against CD44 (Figure 5.8b) we saw a greater inhibition of VLS in the lung and liver. These data further supported a role for CD44 in the induction of VLS.

IL-2 administration increases $CD8^+$ T cells and decreases $CD4^+$ T cells in the spleen: We investigated the effect of IL-2 treatment on T cell populations in wild-type and CD44-ko mice. To this end, T cells were purified from wild-type (+/+) and CD44KO mice treated with IL-2 as described in Figure 5.4, and stained for CD4 and CD8 expression. We found that IL-2 treatment caused an increase in the percentage of $CD8^+$ T cells and a decrease in the percentage of $CD4^+$ T cells in the periphery of wild-type and CD44-ko mice (data not shown).

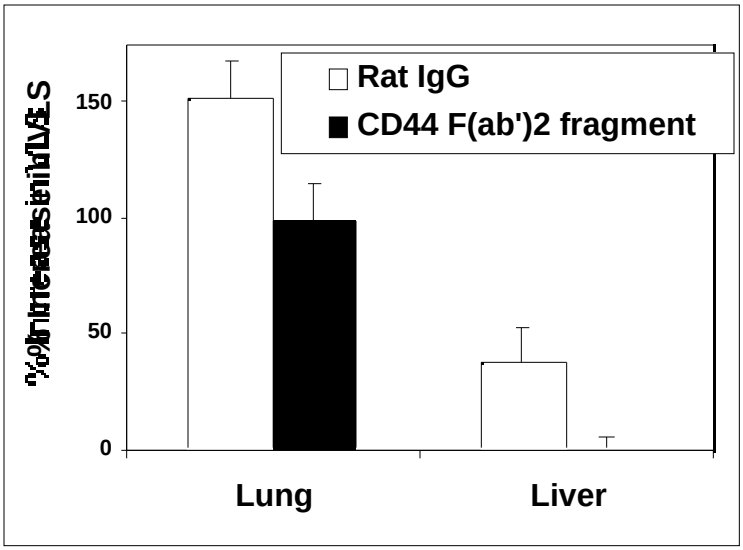

Figure 5.8A: Effects of $F(ab')_2$ Fragments of antibodies against CD44 to block VLS induction in wild-type mice: Groups of 5 mice of C57BL/6 wild-type (+/+) mice were injected with PBS or IL-2 as described in Fig. 4. The IL-2 injected mice in addition received 100 µg of $F(ab')_2$ fragments of anti-CD44 mAbs/mouse/day. As a control, the IL-2 treated mice received 100 µg of normal rat IgG/mouse/day.

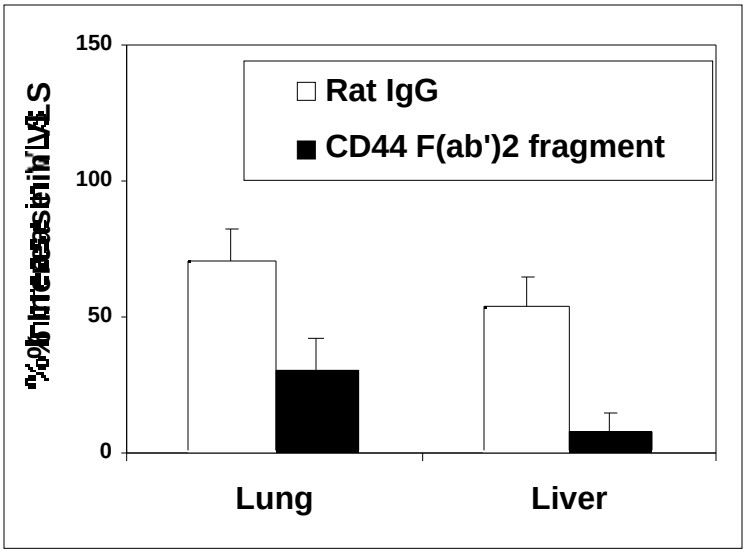

Figure 5.8B: Effects of $F(ab')_2$ Fragments of antibodies against CD44 to block VLS induction in wild-type mice: Groups of 5 mice of C57BL/6 wild-type (+/+) mice were injected with PBS or IL-2 as described in Fig. 5.4. The IL-2 injected mice in addition received 500 µg of $F(ab')_2$ fragments of anti-CD44 mAbs/mouse/day. As a control, the IL-2 treated mice received 500 µg of normal rat IgG/mouse/day.

Decreased LAK activitiy in CD44-KO mice: We investigated the LAK activity in CD44-KO mice. Splenic T cells were cultured with IL-2 and after 48 hours we tested LAK activity against P815, a NK- resistant target cell. We noted that IL-2 activated LAK cells from CD44-KO mice exhibited decreased ability to kill P815 when compared to the wild-type mice (Figure 9).

Discussion

In the current study we observed that IL-2-induced VLS in the lungs and liver was markedly decreased in CD44-KO mice when compared to the wild-type mice. Furthermore, ultrastructural studies demonstrated that unlike the IL-2 injected wild-type mice, CD44-KO mice failed to exhibit endothelial cell damage. These data together demonstrated that CD44 is actively involved in the induction of VLS by IL-2. The fact that administration of $F(ab')_2$ fragments of anti-CD44 mAbs could block the VLS, further corroborated the role played by CD44 in VLS induction. These data also suggested that blocking CD44 may serve as a useful therapeutic approach to prevent endothelial cell injury in a variety of clinical conditions.

There are many disease models in which factors other than cytolytic lymphocytes have been shown to participate in endothelial cell injury, including neutrophils and complement components. (Ward, 1996). However, there is growing evidence for the involvement of cytolytic lymphocytes in endothelial cell injury. For example, IL-2 activated T cells and other leukocytes have been shown kill endothelial cells (Damle et al., 1987; Hammond-McKibben et al., 1995; Damle et al., 1989; Bechard et al., 1989; Fujita et al., Hammond-McKibben et al., 1995). Also, IL-2 induced VLS is seen only in immunocompetent but not nude or immunodeficient mice (Rosenstein et al., 1986; Ettinghausen et al., 1988). Furthermore, depletion of NK/LAK cells in vivo led to decreased toxicity during IL-2 therapy. Studies from our lab demonstrated that administration of a CTL clone plus IL-2 into irradiated

syngeneic mice, but not the CTL clone or IL-2 alone, triggered VLS (Hammond-McKibben et al., 1995). Moreover, we have demonstrated that perforin-deficient or FasL-defective mice exhibit decreased VLS in the lungs and liver following IL-2 therapy (Rafi et al., 1998). Although all of the studies mentioned above indicate the role of cytotoxic lymphocytes in endothelial cell injury and consequent induction of VLS, the exact mechanism of endothelial cell damage is not clear.

We and others have shown that activated CTL, NK cells and the double-negative T cells mediate efficient lysis of target cells when activated through CD44 (Hammond-McKibben et al., 1996; Seth et al., 1991; Galandrini et al., 1993; Tan et al., 1993). Inasmuch as, endothelial cells express the ligands for CD44, it is likely that dysregulated interaction between cytotoxic lymphocytes and endothelial cells can cause endothelial cell lysis. The current study supports this hypothesis. IL-2 treatment activates the LAK cells to express higher levels of perforin and FasL as well as CD44 which may account for their ability to migrate to various organs and cause endothelial cell lysis (Bradely et al., 1998).

It is likely that CTL/LAK-induced endothelial cell damage may occur at sites of chronic inflammation or following cytokine therapy, but not during normal immune responses. This can be explained by regulatory mechanisms operating *in vivo*, during the normal immune response. First, CD44 expression is up-or down-regulated based on the stage of activation of lymphocytes. Secondly, CD44 is expressed in a variety of isoforms and therefore the isoforms involved in cytotoxicity, homing and adhesion may be different. CD44 and its ligand HA is found in soluble form in the serum and known to vary during disease conditions. Such molecules may regulate the interactions between CTL and endothelial cells. Lastly, the interaction between FasL and Fas expressed on cytotoxic lymphocytes and endothelial cells may regulate the degree of nonspecific cytotoxicity *in vivo*.

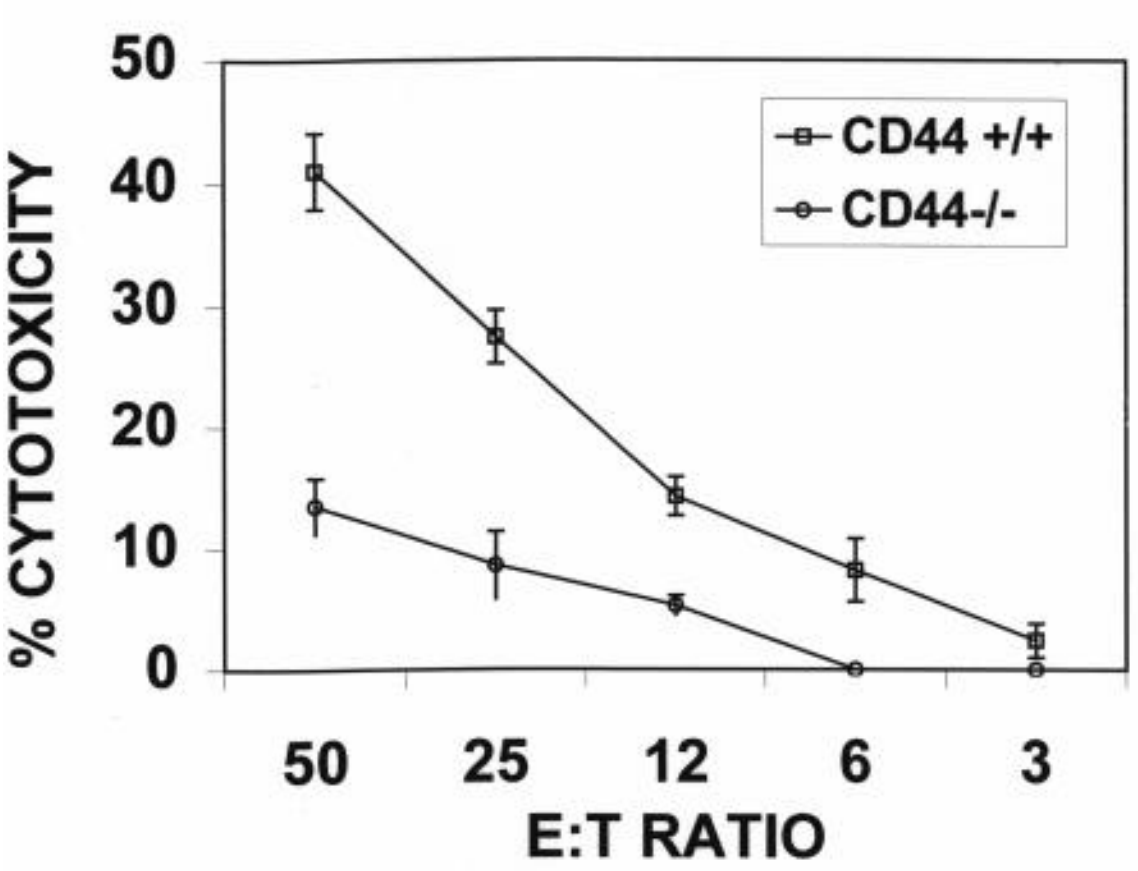

Figure 5.9: LAK activity in CD44+/+ and CD44-/- mice against P815 cell target: Splenic T cells from CD44+/+ and CD44-KO mice were cultured with IL-2 for 48 hours and tested for cytotoxicity against ^{51}Cr-labelled P815. The data indicate mean percent cytotoxicity triplicate cultures±S.E.

Although CD44 is known to play a wide role variety of roles, mice deficient in CD44 do not exhibit developmental or neurological defects. However such mice exhibit decreased LAK cell activity (Matsumoto et al., 1998). This observation was confirmed in the current study in which we noted that IL-2 activated LAK cells from CD44 mice, when compared to the wild-type mice exhibited marked decrease in their ability to kill NK-resistant P815 target cells (Figure 9). In the current study we noted that the IL-2 treated CD44-KO exhibited similar levels of perivascular infiltration with lymphocytes in the lungs and liver when compared to the wild-type mice. These data together suggested that the decreased VLS in CD44-KO mice resulted from inability to mediate lysis of endothelial cells rather than inability of lymphocytes to migrate and home to various organs. This was further corroborated by ultrastructural studies in which endothelial cells from CD44-KO mice showed normal morphology unlike similar cells from wild-type mice which exhibited marked damage. Recent studies have suggested that CD44 expressed by LAK cells may recognize HA on target cells to mediate cytotoxicity (Matsumoto et al., 1998). In an earlier study we noted that B lymphocytes when activated with HA underwent proliferation and differentiation (Rafi et al., 1997). In the current study, we used CD44-KO mice to test whether such cells would exhibit decreased response to HA. The data demonstrated that the B cell responsiveness to HA in CD44-KO mice was significantly diminished, but not completely abrogated. These data further confirmed the role of CD44-hyaluronate interaction in lymphocyte activation. Also, since the responsiveness of B cells to HA in CD44-KO mice was not completely abrogated, alternate receptors such as CD38 (Nishina et al., 1994) may play a role in B cell activation.

In the current study, although IL-2 induced VLS was used as a model to study endothelial cell damage, there are a number of clinical diseases in which similar endothelial cell injury has been reported. In murine lymphocytic choriomeningitis (LCM) viral infection massive delayed-type hypersensitivity

(DTH) reaction has been known to occur in the nervous system, caused by $CD8^+$ T cells (Doherty et al., 1990). It has been speculated that virally activated $CD8^+$ T cell expressing high levels of CD44, kill endothelial cells leading to massive extravasation of monocytes and $CD4^+$ T cells in the subarachnoid space. In autoimmune disease models involving vasculitides, the lesions are associated with infiltration of lymphocytes and macrophages at the vascular wall structure (Moyer et al., 1984). The T cell involvement in the endothelial cell damage also leads to vascular disease in scleroderma (Kahaleh et al., 1990). The peripheral blood lymphocytes from some patients with rheumatoid arthritis and giant cell arthritidis have been shown to be cytotoxic to endothelial cells, but not to fibroblasts (Blann et al., 1991). Further studies in such disease models on the role of CD44 should help in understanding and preventing pathogenesis.